Reaction Kinetics of CO2 Carbonation with Mg-Rich Minerals

ARTICLE *in* THE JOURNAL OF PHYSICAL CHEMISTRY A · JUNE 2011

Impact Factor: 2.69 · DOI: 10.1021/jp2040899 · Source: PubMed

THE JOURNAL OF PHYSICAL CHEMISTRY A

ARTICLE

pubs.acs.org/JPCA

Reaction Kinetics of CO_2 Carbonation with Mg-Rich Minerals

Soonchul Kwon,[†] Maohong Fan,[*,‡,†] Herbert F. M. Dacosta,[§] Armistead G. Russell,[†] and Costas Tsouris[∥]

[†]Georgia Institute of Technology, Atlanta, Georgia 30332, United States

[‡]University of Wyoming, Laramie, Wyoming 82071, United States

[§]Chem-Innovations, P.O. Box 3665, Peoria, Illinois 61612, United States

[∥]Oak Ridge National Laboratory, Oak Ridge, Tennessee 37831, United States

ABSTRACT: Due to their low price, wide availability, and stability of the resulting carbonates, Mg-rich minerals are promising materials for carbonating CO_2. Direct carbonation of CO_2 with Mg-rich minerals reported in this research for the first time could be considerably superior to conventional liquid extraction processes from an energy consumption perspective due to its avoidance of the use of a large amount of water with high specific heat capacity and latent heat of vaporization. Kinetic models of the reactions of the direct CO_2 carbonation with Mg-rich minerals and within simulated flue gas environments are important to the scale-up of reactor designs. Unfortunately, such models have not been made available thus far. This research was initiated to fill that gap. Magnesium silicate (Mg_2SiO_4), a representative compound in Mg-rich minerals, was used to study CO_2 carbonation reaction kinetics under given simulated flue gas conditions. It was found that the chosen sorbent deactivation model fits well the experimental data collected under given conditions. A reaction order of 1 with respect to CO_2 is obtained from experimental data. The Arrhenius form of CO_2 carbonation with Mg_2SiO_4 is established based on changes in the rate constants of the chosen deactivation model as a function of temperature.

$$k = 2.3\times10^{6} e^{-\frac{5{,}193}{T}} \ (\mathrm{kmol^{6}\cdot kg\cdot min})$$

$$k_d = 2.5\times10^{6} e^{-\frac{5{,}837}{T}} \ (\mathrm{L/min})$$

INTRODUCTION

The concentration of CO_2 in the atmosphere has been continuously increasing for many years due to the emissions of CO_2 from many sources.[1,2] About 40% of the total emissions of CO_2 in the U.S. are generated by power plants that use fossil fuels including coal, natural gas, and oil as their major energy sources. In the recent years, various technologies have been developed to capture CO_2.[3−13] The costs associated with the current CO_2 capture technologies are too high to be widely accepted. Without an economically viable CO_2 capture technology, carbon capture and storage (CCS) cannot be justified.[14] CO_2 capture by adsorption does not appear to be thermodynamically limited and, because of the possibility of high CO_2 selectivity and low energy demand,[15] adsorption appears to be one of the more promising options among the various technologies proposed for capturing CO_2 from power plant flue gases. Consequently, the development of economical and effective adsorbents is desirable. Solid sorbents are an attractive choice because they are easy to handle, are not associated with a risk of releasing solvents in the environment, have low deployment costs, and cause negligible corrosion problems. Further, they cause lower environmental impacts.[16,17]

Flue gases from power plants typically contain 8−12% (vol) CO_2 and 8−10% steam (H_2O). Due to the tendency of H_2O molecules to also be adsorbed by the sorbent, many sorbents lose their CO_2 adsorption capacities in the presence of water vapor.[18] Accordingly, sorbents with high adsorption capacities for CO_2 in the presence of water are desirable for their practical applications in power plants. Therefore, it is important to identify solid sorbents whose CO_2 sorption capacities are not negatively affected due to the presence of water vapor.

Because of their low price, wide availability, and the fact that their CO_2 adsorption capacity and rate increase in the presence of H_2O, magnesium-rich (Mg-rich) minerals are promising candidates for CO_2 separation.[19−21] Due to the fact that CO_2 is captured as a stable carbonate, mineral-based CO_2 removal processes can minimize the risk of CO_2 leakage compared to other methods, thereby providing the potential for long-term CO_2 sequestration. Moreover, solid byproducts from the CO_2 mineralization process have many potential applications, including soil remediation.[21] However, even though their associated reactions are thermodynamically favorable, natural Mg-rich, mineral-based carbonation processes are slow because of the low surface area available.[19,21,22] Therefore, researchers have shown increasing interest in improving the kinetics of mineral-based, Mg-rich CO_2 carbonation methods. One approach is to use an aqueous extraction process under elevated pressure and temperature that can improve the kinetics of reaction between Mg_2SiO_4 and CO_2. However, because it requires either mechanical or chemical pretreatment of Mg-rich minerals, this process is indirect and overly time-consuming.

By contrast, not only might the use of Mg-rich minerals for the direct carbonation of CO_2 in flue gases overcome certain shortcomings of an aqueous extraction process, it might also help to identify methods for improved rates of capture. However, to the authors' knowledge, studies on kinetic models

Received: May 3, 2011
Revised: May 28, 2011
Published: May 31, 2011

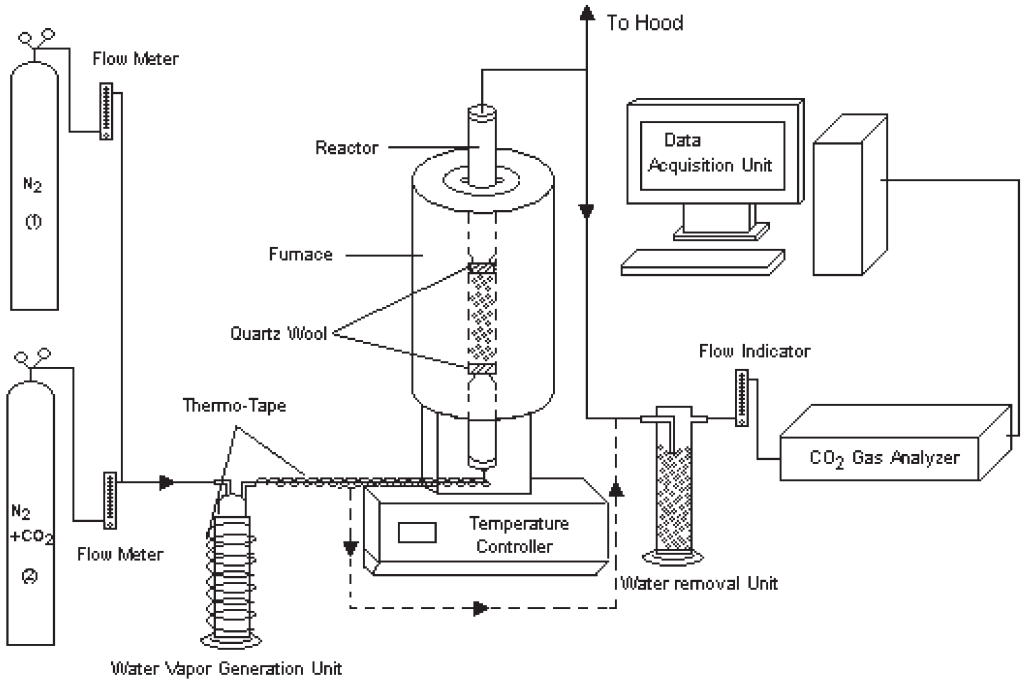

Figure 1. Schematic diagram of experimental setup for Mg_2SiO_4-based CO_2 sorption.

of the reactions between Mg-rich minerals and gaseous CO_2 within a simulated flue gas environment, including rate equation and Arrhenius form, have not yet been reported. Thus, the development of kinetic models for the early application of Mg-rich CO_2 carbonation in coal-fired power plants is desirable.

Pure magnesium silicate (Mg_2SiO_4) was selected in this research to study the kinetics of the reaction between Mg-rich minerals and CO_2 within a simulated flue gas environment. The overall reaction between Mg_2SiO_4 and H_2O is

$$^1/_2 Mg_2SiO_4 + CO_2 \overset{H_2O}{\rightleftharpoons} MgCO_3 + {}^1/_2 SiO_2 \qquad (R1)$$

Mg_2SiO_4 is chosen as a model CO_2 sorbent because it represents major Mg-rich minerals existing in nature (e.g., olivine and serpentine) and because the use of a single compound simplifies the kinetic study.

EXPERIMENTAL SECTION

Materials. Mg_2SiO_4 was supplied by Alfa Aesar and used without further treatment. Mg_2SiO_4 is in the form of a white powder with 99% purity, a median particle size of 3.5 μm, and a bulk density of 3.21 g/cm^3. The X-ray diffraction (XRD) patterns of the Mg_2SiO_4 both before and after carbonation were analyzed using an X'PERT model X-ray diffractometer (Philips), with Cu Kα as the radiation resource, and with scans performed in the 2θ range from 5° to 95° with 0.02°/s.

Experimental Apparatus. The schematic of the experimental setup for CO_2 capture (Figure 1) consists of three parts: a flue gas simulation unit, a CO_2 sorption system, and CO_2 analysis equipment. Gas cylinders containing pure N_2 and a mixture of CO_2 and N_2 with a flow rate of 0.5 L/s were used to conduct all tests. Flow rates of the feed gases were manually controlled with Matheson Trigas FM-1050 flowmeters. An additional flowmeter was used to determine if the flow of the inlet gas analyzer was normal during all CO_2 sorption operations.

Adsorption of CO_2 with Mg_2SiO_4 was carried out in a quartz tubular reactor with a length of 610 mm and inside diameter of 9 mm. The fixed sorbent bed in the reactor was formed by placing the Mg_2SiO_4 particles between two pieces of quartz wool to serve as bed holders. The quartz reactor was placed inside a TF55030A-1 tube furnace (Thermo Corporation, Asheville, NC), with a UT150 temperature controller (Yokogawa M&C Corp., Newnan, GA) to control the CO_2 sorption temperature. The CO_2 sorption unit was connected to a steam generation unit to introduce water into the simulated dry flue gas stream containing CO_2 and N_2. In order to avoid steam condensation prior to the flow of the simulated wet flue gas into the sorbent bed, thermotape was used to wrap the pipelines between the vapor injection point and the inlet gas-reactor connection, with temperature controllers employed to control the heating rates of the thermotape. The outlet gas from the tubular reactor was passed through a steam removal unit before entering the ZRE gas analyzer (California Analytical Instruments, Inc.), where the CO_2 concentration was measured. The CO_2 concentration in the simulated dry flue gas stream was also measured before each sorption test started. A data acquisition system was connected directly to the gas analyzer in order to continuously record measured CO_2 concentrations.

Operating Procedures. The CO_2 adsorption capacity of Mg_2SiO_4 under a given condition was determined based on changes in measured CO_2 concentrations after adsorption. Each test run was conducted with fresh Mg_2SiO_4. First, 0.50 g of Mg_2SiO_4 was lightly packed into the tubular reactor, which was preheated for 10 min to ensure constant operating conditions at the desired reaction temperature. The tubular reactor was then connected to the gas supply unit and the gas analyzer. At the same time, the data acquisition unit was turned on. The

dx.doi.org/10.1021/jp2040899 |J. Phys. Chem. A 2011, 115, 7638–7644

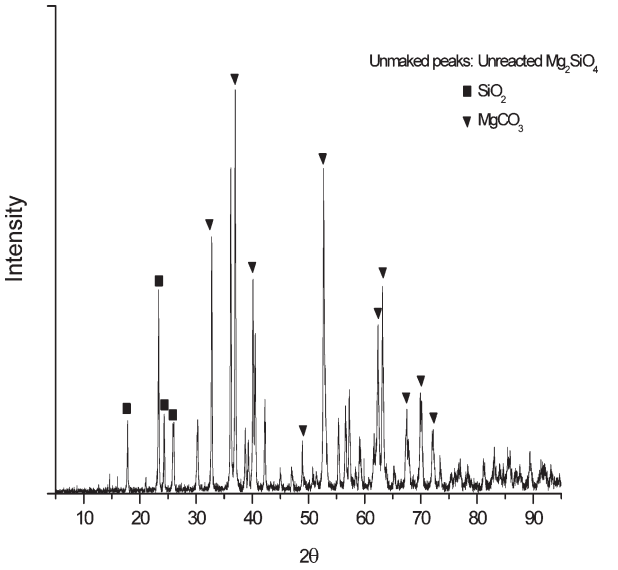

Figure 2. XRD patterns of spent Mg_2SiO_4 [(inlet gas conditions, H_2O, 4.1 mmol/L; CO_2, 4.1 mmol/L; total gas flow rate, 0.5 L/min); weight of Mg_2SiO_4, sorption temperature, 150 °C].

composition of effluent gas from the steam removal unit was measured immediately by the ZRE gas analyzer. When the CO_2 concentration in the effluent gas stream was within 1% of the initial inlet gas-stream concentration (indicating that the Mg_2SiO_4 particle surfaces were saturated with CO_2), the flow of simulated flue gas into the reactor was stopped. Each reported data point in this study represents the average value of three tests under the same operating conditions.

RESULTS AND DISCUSSION

Determination of the Temperature Range for Kinetic Study. Thermodynamic calculations have shown that the Gibbs free energy changes of (R1) are −32.95, −20.88, and −3.88 kJ/mol at temperatures of 25, 100, and 200 °C, respectively, indicating that Mg_2SiO_4-based CO_2 mineralization should occur in the given temperature range, which is supported by the results (Figures 2 and 3). CO_2 adsorption occurred on the surface of Mg_2SiO_4 at 200 °C, as demonstrated by the peaks of carbonation products ($MgCO_3$ and SiO_2) of (R1) (Figure 2), a finding consistent with the observations of other researchers.[20,23,24]

The increase in the Gibbs free energy changes of (R1) with temperature signifies that higher temperatures could have considerable negative effects on the thermodynamics of CO_2 on Mg_2SiO_4. On the other hand, the rate of reaction improves at higher temperatures. Therefore, an appropriate temperature range should be chosen for study of the reaction kinetics of (R1). Our preliminary tests showed that the reaction rate of (R1) was quite slow in the temperature range of 0−100 °C, even though the sorbent could achieve reasonably large CO_2 sorption capacities over very long sorption periods. However, given that the volume of the emitted CO_2-containing flue gas is so large, slow sorption would require the construction of very bulky adsorber units to extend considerably the time of contact between Mg_2SiO_4 and CO_2 in order to achieve high CO_2 capture efficiencies, a prohibitively expensive approach.

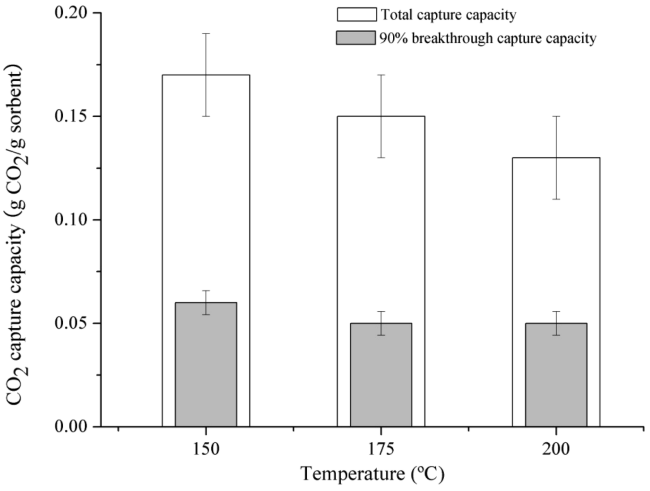

Figure 3. Total and breakthrough CO_2 sorption capacities of Mg_2SiO_4 at different temperatures [(inlet gas conditions, H_2O, 4.1 mmol/L; CO_2, 4.1 mmol/L; total gas flow rate, 0.5 L/min); weight of Mg_2SiO_4, 0.5 g].

A good sorbent should, therefore, have not only a high total sorption capacity but also a high breakthrough capacity. High breakthrough capacity is determined by inherent characteristics of the sorbent, including molecular structure, pore structure, surface defect or active site, BET (Brunauer, Emmett and Teller) surface area, and sorption operation conditions. Since it is directly related to the reaction kinetics of (R1), temperature is expected to be one of the more important operational factors affecting the breakthrough capacity of Mg_2SiO_4. The total and breakthrough CO_2 sorption capacities of Mg_2SiO_4 at 150, 175, and 200 °C (Figure 3) show that, compared to other solid sorbents, Mg_2SiO_4 has good CO_2 sorption performance at the three temperatures.[25−31] While the total sorption capacity of Mg_2SiO_4 decreases with an increase in temperature, the breakthrough capacity does not change considerably (Figure 3). Our tests showed that the breakthrough sorption capacity achieved at 150 °C, when CO_2 separation efficiencies were close to 100%, was lower than that obtained at 200 °C. Further, the ratio of breakthrough sorption capacity to the total sorption capacity increased with temperature under the given experimental conditions (Figure 3) and was higher than those of most of the reported sorbents.[31−36] Because its performance in the 150−200 °C range suggests that Mg_2SiO_4 could react with CO_2 reasonably fast and with a considerable CO_2 sorption capacity, a 100−200 °C temperature range was chosen to study the kinetics of reaction between Mg_2SiO_4 and CO_2.

Sorption Kinetics. *Determination of Reaction Order and Rate Constants.* Park[37] successfully used a deactivation model to describe the decrease in activity of Na_2CO_3 during reaction of NaOH with CO_2. Because the heterogeneous CO_2 adsorption process investigated in this research is very similar to that of Park's,[37] his deactivation model is used to establish the rate equation of (R1).

According to the deactivation model, Mg_2CO_3 forms gradually during the carbonation process and covers the surface of Mg_2SiO_4, thus reducing the activity or carbonation rate of the sorbent. Assuming that the pseudo-steady-state hypothesis is applicable within a constant water vapor concentration environment, the deactivation equation of the Mg_2SiO_4-based CO_2 carbonation process in a packed bed reactor shown in Figure 1

can be expressed as[37]

$$a = \frac{C_{CO_2}}{C_{CO_2,0}} = \exp\left[\frac{\left[1-\exp\left(\frac{kC_{H_2O}W_{Mg_2SiO_4}}{Q_g}\right)(1-\exp(-k_d t))\right]}{1-\exp(-k_d t)}\exp(-k_d t)\right] \quad \text{(E1)}$$

or

$$C_{CO_2} = C_{CO_2,0}\exp\left[\frac{\left[1-\exp\left(\frac{kC_{H_2O}W_{Mg_2SiO_4}}{Q_g}\right)(1-\exp(-k_d t))\right]}{1-\exp(-k_d t)}\exp(-k_d t)\right] \quad \text{(E2)}$$

where $C_{CO_2,0}$ and C_{CO_2} are the inlet and outlet concentrations (kmol/m^3) of CO_2 in the gas stream, respectively, at any sorption time (t) and k is the initial sorption rate constant [m^6/(kmol·kg·min)] in the following CO_2 isothermal conservation equation

$$-Q_g\frac{dC_{CO_2}}{dw_{Mg_2SiO_4}} - kC_{H_2O}C_{CO_2}^{n(CO_2)}\alpha_{Mg_2SiO_4}^{m(Mg_2SiO_4)} = 0 \quad \text{(E3)}$$

Here, C_{H_2O} is the concentration of water vapor (kmol/m^3), $W_{Mg_2SiO_4}$ is the weight of Mg_2SiO_4 (kg) in the reactor, Q_g is the volumetric flow rate of the inlet gas mixture (L/min), $w_{Mg_2SiO_4}$ is consumed Mg_2SiO_4, n_{CO_2} is the reaction order with respect to CO_2, $m_{Mg_2SiO_4}$ is the power of $\alpha_{Mg_2SiO_4}$ (the activity of Mg_2SiO_4 defined as $(W_{Mg_2SiO_4} - w_{Mg_2SiO_4})/W_{Mg_2SiO_4}$, varying from 0 to 1), and k_d is the deactivation rate constant [m^3/(kmol·min)] when n_{CO_2} and $m_{Mg_2SiO_4}$ are 1 in the following sorbent deactivation equation

$$-\frac{d\alpha_{Mg_2SiO_4}}{dt} = k_d C_{CO_2}^{n(CO_2)}\alpha_{Mg_2SiO_4}^{m(Mg_2SiO_4)} \quad \text{(E4)}$$

The choices for $n_{CO_2} = 1$ and $m_{Mg_2SiO_4} = 1$ are based on Park's studies[37] on the Na_2CO_3 reaction system, which is very similar to the one studied in this research. An iterative method was used to determine k and k_d at a given temperature. The k and k_d ultimately chosen should make the C_{CO_2} vs t relationship predicted by (E2) under given experimental conditions match the C_{CO_2} vs t profiles recorded by the CO_2 analyzer, as shown in Figure 4, for the results obtained at a given temperature under different flow rates. The differences of the two C_{CO_2} vs t relationships, shown in Figure 4 to become larger after a period of reaction time will be explained in one of the following paragraphs.

We chose to use the sorption profile obtained at 200 °C (Figure 4) to test the deactivation model (E2), since the slope resolution of the sorption profile at 200 °C is higher than that at other temperatures due to the increases of k and k_d with temperature. On the basis of the assumption that $n_{CO_2} = 1$ and $m_{Mg_2SiO_4} = 1$ at 200 °C, and under other given reaction conditions, (E4) can be written as

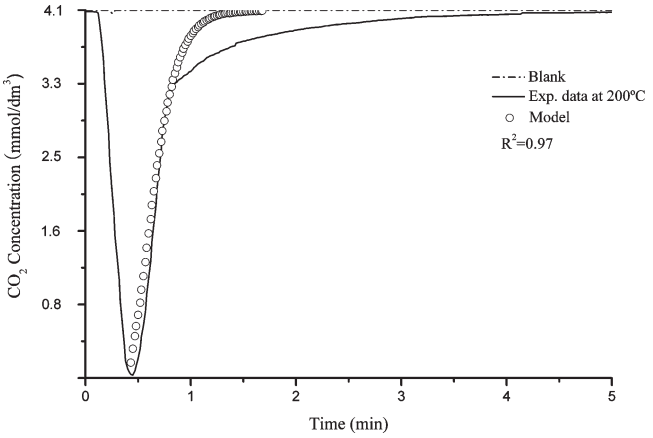

Figure 4. Mg_2SiO_4 based CO_2 sorption profile at 200 °C [(inlet gas conditions, H_2O, 4.1 mmol/L; CO_2, 4.1 mmol/L; total gas flow rate, 0.5 L/min); weight of Mg_2SiO_4, 0.5 g].

$$-\frac{d\alpha_{Mg_2SiO_4}}{dt} = k_d C_{CO_2}\alpha_{Mg_2SiO_4} \quad \text{(E5)}$$

If the rate-limiting reaction in the overall reaction mechanism of (R1) does not change within the range of 100−200 °C, $m_{Mg_2SiO_4}$ and n_{CO_2} should not vary either, and their values can therefore be obtained with the sorption data collected at any temperature within the range. However, $m_{Mg_2SiO_4} = 1$ and $n_{CO_2} = 1$ are assumed values and were tested only under limited test conditions. Thus, their applicability within broader ranges of test conditions should be further supported with theoretical derivations, as discussed below.

Assuming (R1) proceeds through the following elementary steps in the presence of water during the CO_2 sorption process

$$CO_2 + H_2O \leftrightarrow 2H^+ + CO_3^{2-} \quad \text{(R2)}$$

$$^1/_2 Mg_2SiO_4 + 2H^+ \rightarrow Mg^{2+} + H_2O + {}^1/_2 SiO_2 \quad \text{(R3)}$$

$$Mg^{2+} + CO_3^{2-} \rightarrow MgCO_3 \quad \text{(R4)}$$

(R2) is a reversible reaction that can reach its equilibrium state quickly, leading to

$$k_{(R2),forward}C_{CO_2}C_{H_2O} - k_{(R2),reverse}C_{net,H^+}^2 C_{net,CO_3^{2-}} = 0 \quad \text{(E6)}$$

or

$$C_{net,H^+}^2 = \frac{k_{(R2),forward}}{k_{(R2),reverse}}\frac{C_{CO_2}C_{H_2O}}{C_{net,CO_3^{2-}}} \quad \text{(E7)}$$

where $k_{(R2),forward}$ and $k_{(R2),reverse}$ represent the forward and reverse reaction rate constants of (R2), respectively, and C_{CO_2} and C_{H_2O} correspond to the concentrations of CO_2 and H_2O, respectively. Since H_2O is actually neither consumed nor generated when both (R2) and (R3) are considered, C_{H_2O} can be treated as a constant. H_2O is simply an indispensible H^+ carrier. C_{net,H^+} is the net concentration of H^+, which is the sum of the concentrations of the H^+ generated from the forward reaction of (R2) and the H^+ consumed by (R4) and the reverse reaction of (R2).

dx.doi.org/10.1021/jp2040899 |J. Phys. Chem. A 2011, 115, 7638–7644

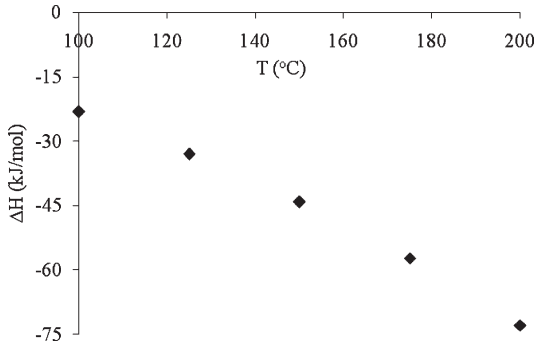

Figure 5. Effect of temperature on enthalpy change of CO_2 hydrolysis.

$C_{net,CO_3^{2-}}$ is the net concentration of CO_3^{2-}, which is the sum of the concentrations of the CO_3^{2-} generated from the forward reaction of (R2) and the CO_3^{2-} consumed by (R4) and the reverse reaction of (R2). According to the pseudo-steady-state theory,[38] $C_{net,CO3}^{2-}$ can be treated as a constant. Furthermore, $C_{net,CO3}^{2-}$ should be low for two reasons. First, since exothermal characteristics of the reaction (Figure 5) result in CO_2 having low solubility in water in the tested temperature range (particularly at 200 °C, a relatively high temperature for sorption), the forward reaction rate of (R2) is slow. Therefore, (R2) or the interaction between H_2O and CO_2 is the rate-controlling step of the overall CO_2 sorption process. Second, given that high pressure is not used, (R3) and (R4) should be much quicker than the forward reaction of (R2), leading to quick consumption of (R2)'s slowly generated CO_3^{2-}. Thus, $C_{net,CO3}^{2-}$ can be considered to be a small constant.

On the basis of (R3), a decrease of $\alpha_{Mg_2SiO_4}$ with time can be expressed as

$$-\frac{d\alpha_{Mg_2SiO_4}}{dt} = k_{(R3)} C_{net,H^+}^2 \alpha_{Mg_2SiO_4}^{0.5}$$

$$= k_{(R3)} \frac{k_{(R2),forward}}{k_{(R2),reverse}} \frac{C_{CO_2} C_{H_2O}}{C_{net,CO_3^{2-}}} \alpha_{Mg_2SiO_4}^{0.5}$$

$$= \frac{k_{(R2),forward} k_{(R3)}}{k_{(R2),reverse}} \frac{C_{H_2O}}{C_{net,CO_3^{2-}}} C_{CO_2} \alpha_{Mg_2SiO_4}^{0.5}$$

$$= k' C_{CO_2} \alpha_{Mg_2SiO_4}^{0.5} \quad \text{(E8)}$$

where

$$k' = \frac{k_{(R2),forward} k_{(R3)}}{k_{(R2),reverse}} \frac{C_{H_2O}}{C_{net,CO_3^{2-}}}$$

is a constant. Comparing (E8) to (E5), we find that the reaction orders with respect to CO_2, i.e., $n_{CO_2,experiment}$ in (E5) and $n_{CO_2,theory}$ in (E8), obtained with experimental results and derived with a postulated reaction mechanism, respectively, are exactly the same. However, $m_{Mg_2SiO_4,experiment} = 1$ in (E5), is larger than $m_{Mg_2SiO_4} = 0.5$ in (E8). In the meantime, $m_{Mg_2SiO_4,experiment} = 1$ still makes (E2) fit the experimental data well at the early stage of sorption. This is because when $\alpha_{Mg_2SiO_4}$ is within 0.85−1, which is the range used in Figure 4 for comparing $C_{CO_2,measured}$ and $C_{CO_2,predicted\ with\ (E2)}$,

$$\left.\frac{\alpha_{Mg_2SiO_4}^{0.5} - \alpha_{Mg_2SiO_4}}{\alpha_{Mg_2SiO_4}^{0.5}} \times 100\%\right|_{maximum}$$

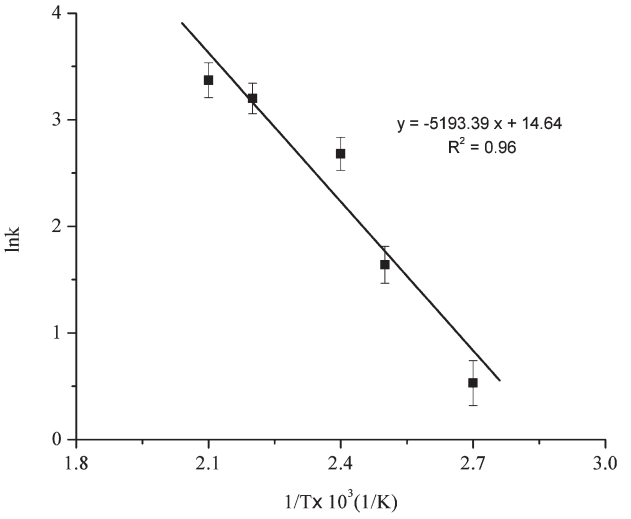

Figure 6. Determination of parameters of Arrhenius form of initial CO_2 sorption [H_2O, 4.1 mmol/dm^3; CO_2, 4.1 mmol/dm^3; total gas flow rate, 0.5 L/min; weight of Mg_2SiO_4, 0.5 g; sorption temperature, 100−200 °C].

is less than 8%. Clearly, when $\alpha_{Mg_2SiO_4}$ continues to decrease, the difference between the assumed $m_{Mg_2SiO_4}$ (1) and the $m_{Mg_2SiO_4}$ (0.5) that was postulated with the reaction mechanism leads to an increase in ($C_{CO_2,predicted\ with\ (E2)} - C_{CO_2,measured}$), as shown in the later CO_2 mineralization stage in Figure 4. Even though an analytical solution or explicit expression of (E1) or (E2) cannot be derived from (E3) and (E4), and numerical methods must be used, it is better to use $m_{Mg_2SiO_4} = 0.5$ in (E3) and (E4) for predicting the Mg_2SiO_4 deactivation rate.

Arrhenius Form. The relationship between rate constants (k or k_d) and reaction temperature (T) can be correlated using the Arrhenius form[38]

$$k = Ae^{-E/RT} \quad \text{(E9)}$$

$$k_d = A_d e^{-E_d/RT} \quad \text{(E10)}$$

where A and A_d are pre-exponential factors treated as constants in the studied temperature range, E and E_d are the activation energy values corresponding to k and k_d, and R is the ideal gas constant. The pre-exponential factors would also be impacted by reactor conditions (e.g., geometry, loading), and these were kept constant between experiments.

The values of k and k_d at 100, 125, 150, and 175 °C were obtained using the same method cited previously for the k and k_d values at 200 °C. The ln k vs T^{-1} and ln k_d vs T^{-1} plots of (R1) are shown in Figure 6 and Figure 7, respectively. Regression found an E value of 43.2 ± 3.7 kJ/mol and an A value of (2.3 ± 0.6) × 10^6 (kmol^6·kg·min), respectively. In addition, regression found an E_d value of 48.5 ± 2.4 kJ/mol and an A_d value of (2.5 ± 0.8) × 10^5 (L/min), respectively. Thus, the Arrhenius forms of CO_2 carbonation with Mg_2SiO_4 within an H_2O environment for the geometry of our experiments are

$$k = 2.3 \times 10^6 e^{5193/T}\ (\text{kmol}^6 \cdot \text{kg} \cdot \text{min}) \quad \text{(E11)}$$

$$k_d = (2.5 \times 10^6) e^{-5837/T}\ (\text{L/min}) \quad \text{(E12)}$$

The reaction order and activation energy of (R1) should not be affected by the flow rate of the simulated flue gas mixture

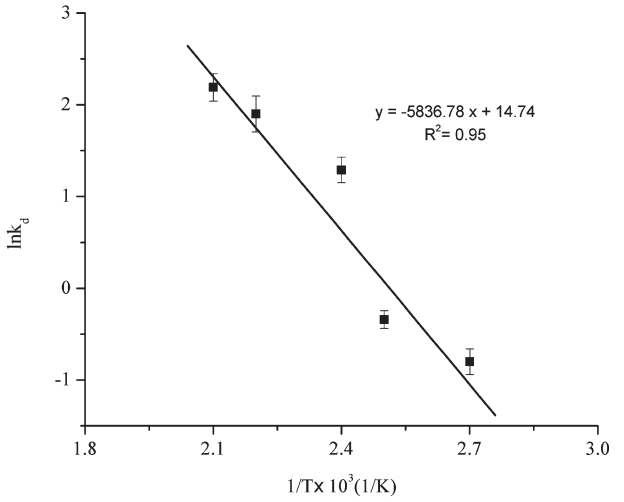

Figure 7. Determination of parameters of Arrhenius form of Mg_2SiO_4 deactivation [H_2O, 4.1 mmol/dm^3; CO_2, 4.1 mmol/dm^3; total gas flow rate, 0.5 L/min; weight of Mg_2SiO_4, 0.5 g; sorption temperature, 100−200 °C].

Table 1. Effect of Gas Flow Rate on Reaction Order and Activation Energy of the Mg_2SiO_4-Based CO_2 Sorption [(inlet gas condition, H_2O, 4.1 mmol/L; CO_2, 4.1 mmol/L; total gas flow rate, 0.5 L/min); weight of Mg_2SiO_4, 0.5 g; sorption temperature, 200 °C]

flow rate (L/min)	initial CO_2 sorption E (kJ/mol)	Mg_2SiO_4 deactivation E_d (kJ/mol)
0.25	42.4 ± 5.1	47.9 ± 4.2
0.5	43.2 ± 3.7	48.5 ± 2.4
1	43.5 ± 4.6	47.2 ± 5.7

under the given CO_2 mineralization conditions, an assumption verified by conducting CO_2 sorption tests with the same initial CO_2 concentration but with gas flow rates of 0.25 and 1.0 L/min. The derived values of E and E_d of (R1) for the three flow rates (0.25, 0.5, and 1.0 L/min) were consistent (see Table 1).

Application Considerations. *Reactor Choice.* Figure 3 shows that the CO_2 breakthrough and total sorption capacities achieved with Mg_2SiO_4 under the given test conditions were in the ranges of 50−60 and 125−175 g of CO_2/kg of Mg_2SiO_4, respectively, which are lower than the theoretical sorption capacity of pure Mg_2SiO_4, 630 g of CO_2/kg of Mg_2SiO_4. Therefore, appropriate measures should be taken to enhance the CO_2 sorption capacities of Mg_2SiO_4 within given reaction conditions, since otherwise a large percentage of Mg_2SiO_4 would be wasted.

One of the conventional methods to increase the chemisorption capacities of sorbents is to improve reaction kinetics, which could theoretically be realized by three approaches for the heterogeneous reaction, i.e., elevation of the reaction temperature, reduction of the particle size of Mg_2SiO_4 or Mg-rich minerals, and an increase in gas pressure.

Since (R1)'s activation energy value (43.2 ± 3.7 kJ/mol) is relatively large, raising the reaction temperature should have a relatively large effect on the reaction rate of the carbonation process. However, since the Gibbs free energy change of (R1) increases with an increase in temperature, any increase in temperature is unfavorable to (R1). Indeed, the reaction becomes unfavorable above 200 °C.

The median particle size of Mg_2SiO_4 used in this research was 3.5 μm, which is already small for fixed-bed reactors. Further reductions in Mg_2SiO_4 particle size can create higher Mg_2SiO_4 surface areas, thereby improving CO_2 breakthrough sorption capacities within a given time period. However, this can also lead to a considerable increase in back pressure, undesirable in fixed-bed reactors because, according to Ergun's equation[39]

$$\Delta P/L = 150\frac{(1-\varepsilon)^2}{\varepsilon^3}\frac{\mu}{{d_p}^2}u + 1.75\frac{1-\varepsilon}{\varepsilon^3}\frac{\rho}{d_p}u^2 \qquad \text{(E13)}$$

where ε is the interparticle porosity of the CO_2 sorption bed, μ is the flue gas viscosity (kg/ms), u is the interstitial velocity (m/s) of the gas stream, ρ is the density (kg/m^3) of flue gas, and $\Delta P/L$ is the pressure drop (Pa/m) of gas in the fixed bed. As shown, $\Delta P/L$ is significantly affected by the particle size of Mg_2SiO_4 (d_p). Accordingly, a fluidized-bed reactor might be used to overcome the stricter particle-size constraints of a fixed bed. The pressure of flue gas should be elevated when fluidized-bed reactors are used. However, use of fluidized-bed reactors does not necessarily entail the increase in the overall CO_2 capture expense due to their advantages over fixed bed reactors.

Other Compounds in Mg-Rich Minerals. Mg-rich minerals in nature often contain other metals in the form of silicates such as Fe_2SiO_4. However, because their concentrations in the minerals are very low, these metals should not have any significant effect on (R1).

SO_x/NO_x. As with any other CO_2 separation technologies, the effects of SO_x/NO_x in flue gas on the studied CO_2 carbonation process should be considered as well. Acids resulting from the hydrolysis of SO_x/NO_x are much stronger than those from CO_2 and thus can react easily with Mg_2SiO_4. However, because their concentrations in flue gas are only at parts per million levels (far lower than the percentage levels of CO_2), and Mg-rich minerals are not intended to be used as regenerated sorbents for CO_2 in the first place, the effects of SO_x/NO_x may be negligible.

AUTHOR INFORMATION

Corresponding Author
*E-mail: mfan@uwyo.edu.

ACKNOWLEDGMENT

This work was supported by Caterpillar, Siemens, and the School of Energy Resources at the University of Wyoming.

REFERENCES

(1) Keeling, C. D.; Whorf, T. P.; Wahlen, M.; Vanderplicht, J. *Nature* **1995**, *375*, 666.
(2) Skinner, L. C.; Fallon, S.; Waelbroeck, C.; Michel, E.; Barker, S. *Science* **2010**, *328*, 1147.
(3) Ma, X. L.; Wang, X. X.; Song, C. S. *J. Am. Chem. Soc.* **2009**, *131*, 5777.
(4) Hicks, J. C.; Drese, J. H.; Fauth, D. J.; Gray, M. L.; Qi, G. G.; Jones, C. W. *J. Am. Chem. Soc.* **2008**, *130*, 2902.
(5) Zhang, B.; Fan, M.; Bland, A. E. *Energy Fuels* **2011**, *25*, 1919.
(6) Fan, G. J.; Wee, A. G. H.; Idem, R.; Tontiwachwuthikul, P. *Ind. Eng. Chem. Res.* **2009**, *48*, 2717.
(7) Tan, J.; Shao, H.-W.; Xu, J.-H.; Du, L.; Luo, G.-S. *Ind. Eng. Chem. Res.* **2011**, *50*, 3966.

(8) Han, B.; Zhou, C.; Wu, J.; Tempel, D. J.; Cheng, H. *J. Phys. Chem. Lett.* **2011**, *2*, 522.
(9) Mansourizadeh, A.; Ismail, A. F.; Matsuura, T. *J. Membr. Sci.* **2010**, *353*, 192.
(10) Wang, X. L.; Dong, H. F.; Zhang, X. P.; Xu, Y.; Zhang, S. J. *Chem. Eng. Technol.* **2010**, *33*, 1615.
(11) Tang, J. B.; Shen, Y. Q.; Radosz, M.; Sun, W. L. *Ind. Eng. Chem. Res.* **2009**, *48*, 9113.
(12) Aaron, D.; Tsouris, C. *Sep. Sci. Technol.* **2005**, *40*, 321.
(13) Page, S. C.; Williamson, A. G.; Mason, I. G. *Energy Policy* **2009**, *37*, 3314.
(14) Tsouris, C.; Aaron, D. S.; Williams, K. A. *Environ. Sci. Technol.* **2010**, *44*, 4042.
(15) Plaza, M. G.; Pevida, C.; Arenillas, A.; Rubiera, F.; Pis, J. J. *Fuel* **2007**, *86*, 2204.
(16) Niswander, R. H.; Edwards, D. J.; Dupart, M. S.; Tse, J. P. *Sep. Sci. Technol.* **1993**, *28*, 565.
(17) Veawab, A.; Tontiwachwuthikul, P.; Chakma, A. *Ind. Eng. Chem. Res.* **1999**, *38*, 3917.
(18) Hiyoshi, N.; Yogo, K.; Yashima, T. *Recent Advances in the Science and Technology of Zeolites and Related Materials, Parts A—C*; Studies in Surface Science and Catalysis, 154; Elsevier: Amsterdam and Boston, 2004; p 2995.
(19) Lin, P. C.; Huang, C. W.; Hsiao, C. T.; Teng, H. *Environ. Sci. Technol.* **2008**, *42*, 2748.
(20) Lackner, K. S.; Wendt, C. H.; Butt, D. P.; Joyce, E. L.; Sharp, D. H. *Energy* **1995**, *20*, 1153.
(21) Maroto-Valer, M. M.; Fauth, D. J.; Kuchta, M. E.; Zhang, Y.; Andresen, J. M. *Fuel Process. Technol.* **2005**, *86*, 1627.
(22) Seifritz, W. *Nature* **1990**, *345*, 486.
(23) Hanchen, M.; Prigiobbe, V.; Storti, G.; Seward, T. M.; Mazzotti, M. *Geochim. Cosmochim. Acta* **2006**, *70*, 4403.
(24) O'Connor, W. K.; Dahlin, C. L.; Rush, G. E.; Gerdemann, S. J.; Penner, L. R.; Nilsen, D. N. "*Aqueous mineral carbonation; mineral availability, pretreatment, reaction parametrics, and process studies*, DOE/ARC-TR-04-002, Office of Process Development, National Energy Technology Laboratory (formerly Albany Research Center), Office of Fossil Energy, US DOE: Washington, DC, 2004.
(25) Bibara, P. J.; Filburn, T. P.; Nalette, T. A. Regenerable Solid Amine Sorbent. Patent 5,876,488, 1999.
(26) Gray, M. L.; Champagne, K. J.; Fauth, D.; Baltrus, J. P.; Pennline, H. *Int. J. Greenhouse Gas Control* **2008**, *2*, 3.
(27) Gray, M. L.; Soong, Y.; Champagne, K. J.; Pennline, H.; Baltrus, J. P.; Stevens, R. W.; Khatri, R.; Chuang, S. S. C.; Filburn, T. *Fuel Process. Technol.* **2005**, *86*, 1449.
(28) Ko, D.; Siriwardane, R.; Biegler, L. T. *Ind. Eng. Chem. Res.* **2003**, *42*, 339.
(29) Ko, D.; Siriwardane, R.; Biegler, L. T. *Ind. Eng. Chem. Res.* **2005**, *44*, 8084.
(30) Na, B. K.; Koo, K. K.; Eum, H. M.; Lee, H.; Song, H. K. *Korean J. Chem. Eng.* **2001**, *18*, 220.
(31) Ochoa-Fernandez, E.; Ronning, M.; Grande, T.; Chen, D. *Chem. Mater.* **2006**, *18*, 6037.
(32) Ochoa-Fernandez, E.; Ronning, M.; Yu, X. F.; Grande, T.; Chen, D. *Ind. Eng. Chem. Res.* **2008**, *47*, 434.
(33) Reynolds, S. P.; Ebner, A. D.; Ritter, J. A. *Adsorption* **2005**, *11*, 531.
(34) Xu, X. C.; Song, C. S.; Miller, B. G.; Scaroni, A. W. *Fuel Process. Technol.* **2005**, *86*, 1457.
(35) Yong, Z.; Mata, V.; Rodrigues, A. E. *J. Chem. Eng. Data* **2000**, *45*, 1093.
(36) Yong, Z.; Mata, V.; Rodriguez, A. E. *Ind. Eng. Chem. Res.* **2001**, *40*, 204.
(37) Park, S. W.; Sung, D. H.; Choi, B. S.; Oh, K. J.; Moon, K. H. *Sep. Sci. Technol.* **2006**, *41*, 2665.
(38) Fogler, H. S. *Elements of Chemical Reaction Engineering*, 4th ed.; Prentice Hall of India: New Delhi, 2006.
(39) Du Plessis, J. P.; Woudberg, S. *Chem. Eng. Sci.* **2008**, *63*, 2576.